Applied Catalysis B: Environmental 98 (2010) 79–85

Contents lists available at ScienceDirect

Applied Catalysis B: Environmental

journal homepage: www.elsevier.com/locate/apcatb

Hydrodechlorination of dichloromethane with a Pd/AC catalyst: Reaction pathway and kinetics

Zahara M. de Pedro*, Jose A. Casas, Luisa M. Gomez-Sainero, Juan J. Rodriguez

Ingeniería Química, Facultad de Ciencias, Universidad Autónoma de Madrid, Cantoblanco, 28049 Madrid, Spain

ARTICLE INFO

Article history:
Received 8 March 2010
Received in revised form 6 May 2010
Accepted 8 May 2010
Available online 13 May 2010

Keywords:
Dichloromethane
Palladium/activated carbon catalyst
Catalytic hydrodechlorination
Kinetic model
Hydrodechlorination mechanism

ABSTRACT

The kinetics of gas-phase hydrodechlorination (HDC) of dichloromethane (DCM) with a Pd on activated carbon commercial catalyst has been studied in a fixed bed reactor within the 200–350 °C temperature range. Different kinetic equations have been checked for describing the evolution of DCM. Statistical and physical reliable parameters were found for a Langmuir–Hinshelwood type expression with DCM adsorption as the controlling step. The reaction pathway and the kinetic model have been elucidated from the evolution of dichloromethane and the identified reaction products (methane, monochloromethane, ethane and ethylene). Adsorbed CH_2Cl^* radical, CH_2^{**} and $C_2H_4^{**}$ carbene species are proposed as the three intermediates evolving to the final reaction products. An apparent activation energy of 23.9 ± 2.3 kJ mol^{-1} has been obtained for dichloromethane disappearance.

1. Introduction

Dichloromethane (DCM) plays an important role in the chemical industry as solvent, dry-cleaner, degreasing agent and adhesive component due to its particular physical and chemical properties, like high volatility and ability to dissolve a wide range of organic compounds. Due to its wide range of industrial applications, dichloromethane is one of the aliphatic organochlorinated compounds released to the atmosphere in greatest quantities in waste gas streams [1]. As it is well known, emissions of organochlorinated pollutants have been progressively restricted in the last years by environmental regulations because of their toxicity, carcinogenic character and potential contribution to the destruction of the ozone layer [2–4]. This leads to the need of developing effective treatment techniques environmentally friendly.

Incineration is a widely used technological option for controlling waste gas emissions. However, halogenated hydrocarbons are combustion inhibitors and high temperatures are needed to achieve high destruction/removal efficiency when dealing with these compounds. Furthermore, formation of harmful highly toxic by-products such as dioxins and furans can occur within a certain temperature range of the off-gas [5,6].

Catalytic hydrodechlorination (HDC) represents one of the most promising emerging technologies with potential economic and environmental advantages respect to incineration for treating waste gases containing organochlorinated compounds [6]. It operates at moderate conditions and the reaction products are much less hazardous [7,8]. Noble metals, such as palladium [9–12], ruthenium [13,14], rhodium [15,16], iridium, rhenium [17], and platinum [18–20] can be expected to catalyze hydrogenolysis of carbon–halogen and they have been tested for hydrodechlorination reactions. Among them, Pd is usually considered as the best catalyst for that process because of its high activity and selectivity towards non-chlorinated products [17,21]. Different supports have been used including activated carbon, alumina, titania, and silica. Activated carbons are potentially attractive supports [22] due to both physical and chemical properties. High dispersion of metallic particles can be achieved using activated carbons with high surface areas and the appropriate surface composition [23,24].

In the last years, several works related to hydrodechlorination of different chlorinated compounds have been published dealing with both chloroaromatics [9,25–29] and chloroaliphatics [30–37]. Nevertheless, probably due to its low reactivity, this reaction has been scarcely studied for DCM.

Most of the existing works focused on DCM hydrodechlorination examine the activity of different catalysts [38–40], the causes of deactivation [28], the differences on reactivity compared to other organochlorinated compounds [41,42], the influence of reaction conditions [31,43] or the effects of the presence of other compounds [44,45]. Nevertheless there is a lack of available kinetic data, which are necessary for reactor design. To the best of our knowledge, the only work dealing with the mechanism of DCM hydrodechlorination was published by Malinowski et al. [46] using

* Corresponding author. Tel.: +34 914973183; fax: +34 914973516.
E-mail addresses: zahara.martinez@uam.es, zahara.martinez@hotmail.com (Z.M. de Pedro).

0926-3373/$ – see front matter © 2010 Elsevier B.V. All rights reserved.
doi:10.1016/j.apcatb.2010.05.007

Nomenclature

a	external surface area per unit of solid-phase volume ($m^2\ m^{-3}$)
C_{DCM0}	initial (inlet) dichloromethane concentration
C_i	exit concentration of species i ($mol\ NL^{-1}$)
Da	Damköhler number, dimensionless
D_{eff}	effective diffusivity of dichloromethane in the catalyst particle (estimated as $Di{\cdot}\varepsilon^2$) ($m^2\ s^{-1}$)
D_i	gas-diffusivity of dichloromethane in nitrogen ($m^2\ s^{-1}$)
d_p	catalyst particle diameter (m)
F_{DCM}	inlet molar flow of dichloromethane ($mol\ h^{-1}$)
k	pseudo-first order kinetic rate constant (h^{-1})
k_1–k_6	kinetic rate constants for the reaction scheme proposed ($NL\ kg^{-1}\ h^{-1}$)
k_a	kinetic rate constant for the Langmuir–Hinshelwood model with dichloromethane adsorption as the rate-controlling step ($NL\ kg^{-1}\ h^{-1}$)
k_d	kinetic constant for the Langmuir–Hinshelwood model with product desorption as the rate-controlling step ($NL\ kg^{-1}\ h^{-1}$)
k_g	mass-transfer coefficient ($m^3\ m^{-2}\ s^{-1}$)
k_i	lumped kinetic rate constant of species i in the kinetic model proposed ($NL\ kg^{-1}\ h^{-1}$)
k_r	kinetic rate constant for the LH model with surface reaction as the rate-controlling step ($NL\ kg^{-1}\ h^{-1}$)
K	lumped equilibrium constant in the kinetic model proposed ($NL\ mol^{-1}$)
K_A	dichloromethane adsorption equilibrium constant for the Langmuir–Hinshelwood model with surface reaction as the rate-controlling step ($NL\ mol^{-1}$)
K_D	product adsorption equilibrium constant for the Langmuir–Hinshelwood model with surface reaction as the rate-controlling step ($NL\ mol^{-1}$)
K_S	lumped equilibrium constant for the Langmuir–Hinshelwood model with dichloromethane adsorption as the rate-controlling step ($NL\ mol^{-1}$)
K_Z	lumped equilibrium constant for the Langmuir–Hinshelwood model with product desorption as the rate-controlling step ($NL\ mol^{-1}$)
L	characteristic length of the catalyst particle (estimated as $d_p/6$) (m)
$(-r_{obs})$	observed reaction rate ($mol\ NL^{-1}\ s^{-1}$)
r_1–r_6	reaction rates according to the reaction scheme proposed ($mol\ kg^{-1}\ h^{-1}$)
r_i	reaction rate of species i ($mol\ kg^{-1}\ h^{-1}$)
R_i	net production rate of species i ($mol\ kg^{-1}\ h^{-1}$)
r^2	correlation coefficient, dimensionless
Re_p	Reynolds number, dimensionless
Sc	Schmidt number, dimensionless
Sh	Sherwood number, dimensionless
W	catalyst weight (kg)
x	conversion, dimensionless

Greek letters

Φ	Wheeler–Weisz number, dimensionless
ε	particle porosity of the Pd/AC catalyst (0.7), dimensionless
ϕ	Thiele modulus, dimensionless
η	catalyst effectiveness factor, dimensionless
τ	space time ($kg\ h\ mol^{-1}$)

a $Pd/\gamma\text{-}Al_2O_3$ catalyst. They suggested the formation of CH_3Cl from CH_2Cl^* adsorbed radical while adsorbed carbene-like and C_1 species evolve to produce CH_4. Readsorption of CH_3Cl or CH_4 was discarded after analyzing the reaction products using D_2 instead of H_2. This is in agreement with the fact that the reactivity of metal surfaces towards hydrodechlorinated products decreases as the chlorine content of the molecule is diminished [42]. Similar conclusions were extracted by Ordoñez et al. [41] who proposed the dissociative adsorption of CH_2Cl_2 onto the metallic surface to produce CH_2Cl^* radical as the first step of DCM hydrodechlorination. On the other hand, there is scarce information about kinetic parameters for DCM hydrodechlorination. Lopez et al. [47] proposed a pseudo-first order kinetic model using a Pd/Al_2O_3 catalyst at low space times and they obtained a value of 24 $mmol\ min^{-1}\ g^{-1}\ MPa^{-1}$ for the rate constant at 250 °C. From differential data, Sanchez et al. [48] reported kinetic rate constant values in the range of 7–14 $L\ g^{-1}\ min^{-1}$ working at 200 °C with Pd at different loads (lower than 1 wt.%) over $\gamma\text{-}Al_2O_3$ and TiO_2.

The aim of this work is to study the kinetics of DCM hydrodechlorination with a commercial Pd on activated carbon (Pd/AC) catalyst. Mass-transfer resistances are previously evaluated and several kinetic models, including those usually found in the literature, are checked for describing the conversion of DCM upon space time in the range of operating conditions tested (temperature of 200–300 °C, space time of 0.2–6.6 $kg\ h\ mol^{-1}$ and a H_2/DCM molar ratio of 100). Based on the experimental results, the reaction pathway is elucidated and a kinetic model is proposed which describes well the evolution of the compounds identified along the process.

2. Experimental

2.1. Materials

The catalyst (0.5 wt.% Pd supported on activated carbon) was supplied by Engelhard Company in reduced state pellets (2.4–4.7 mm).

Hydrogen (99.999%), nitrogen (99.999%) and a commercial mixture of N_2 and dichoromethane (4000 ppmv) were supplied by Praxair.

2.2. Catalyst characterization

N_2 adsorption–desorption (77 K) and mercury porosimetry were used to characterize the porous structure of the catalyst. An Autosorb-1 analyzer (Quantachrome) and a Carlo Erba Porosimeter 4000 were, respectively, employed.

Bulk Pd content was determined by ICP-MS in a Elan 6000 PerkinElmer Sciex system, equipped with an autosampler AS 91. The samples were previously digested with an acids mixture for 15 min in a microwave oven (Milestone MLS 1200 Mega) at 180 °C.

The surface of the catalysts was analyzed by X-ray photoelectron spectroscopy (XPS) with a Physical Electronics 5700C Multitechnique System. The binding energies of the Pd $3d_{5/2}$ core-level and FWHM values were used to asses the chemical state of Pd. Correction for binding energies due to sample charging was effected by taking the C 1s peak (284.6 eV) as an internal standard. The surface Pd content (Pd_{XPS}) was calculated from the area of the spectral peaks.

Table 1 summarizes the characterization of the catalyst.

2.3. Catalytic activity experiments

The hydrodechlorination experiments were conducted in a continuous fixed bed reactor (i.d. = 6.4 mm) provided with temperature, pressure, and gas flow control. Plug flow pattern was assumed since both reactor diameter/catalyst particle diameter and

Table 1
Characterization of the commercial Pd/AC catalyst.

BET surface area ($m^2\,g^{-1}$)	951
External surface area ($m^2\,g^{-1}$)	17
Micropore volume ($cm^3\,g^{-1}$)	0.433
Mesopore volume ($cm^3\,g^{-1}$)	0.017
Macropore volume ($cm^3\,g^{-1}$)	0.133
Pd_{bulk} (wt.%)	0.48
Pd_{XPS} (wt.%)	6.3
$(Pd^0/Pd^{n+}$ molar ratio$)_{XPS}$	1.6

bed length/catalyst particle diameter were higher than 10 and 50, respectively [49]. The reactor was coupled to a gas chromatograph (FID and ECD detectors), for the continuous analysis of the reaction products. A full description of the experimental setup has been reported in a previous paper [43].

Hydrodechlorination runs were carried out at atmospheric pressure using a total flow rate of 100 N mL min^{-1} with the catalyst at a particle size of 0.25–0.50 mm. The gas feed, with a DCM concentration of 1000 ppmv, was prepared by mixing adequate proportions of the starting DCM/N_2 commercial mixture, H_2 and N_2 to obtain a H_2/DCM molar ratio of 100. Space time in the range of 0.2–6.6 kg h mol^{-1} was adjusted by varying the catalyst weight to the desired values. The exit stream from the reactor was periodically analyzed during the first hour once the steady state was reached. That took a short time since previous to each reaction experiment we passed DCM through the bed in absence of H_2 in order to saturate the catalyst. This procedure allowed us to obtain initial conversion values (without catalyst deactivation) and a data reproducibility better than ±5%.

Reaction temperatures within the 200–300 °C range were investigated and isothermal conditions (±1 °C) were facilitated by diluting the catalyst bed with CSi (0.25–0.5 mm).

3. Results and discussion

Previous to the catalytic runs, the contribution of homogeneous reaction (in absence of catalyst) was checked within the 200–350 °C temperature range. No significant DCM conversion (<1%) was achieved.

In a previous work [43] the Pd/AC catalyst showed to be fairly active in the hydrodechlorination of DCM depending on the operating conditions. In order to develop a model capable of describing the intrinsic kinetics of the process, external and internal mass-transfer resistances were evaluated.

A Damköhler (*Da*) dimensionless number was used to evaluate the possible existence of external mass-transfer limitation [50]:

$$Da = \frac{\text{observed reaction rate}}{\text{bulk mass} - \text{transport rate}} = \frac{(-r_{obs})}{k_g a \cdot C_{DCM0}} < 0.1 \quad (1)$$

The observed reaction rate ($-r_{obs}$) was determined from the initial rate method which provides the highest reaction rate values and, therefore, represents the "worst possible scenario". The k_g mass-transport coefficient was calculated from the Frössling correlation [51] which gives the Sherwood number (*Sh*) for spherical particles in a gas flow as a function of Reynolds (Re_p) and Schmidt (*Sc*) numbers:

$$Sh = \frac{k_g d_p}{D_i} = 2 + 0.552 \cdot {Re_p}^{0.53} \cdot Sc^{0.33} \quad (2)$$

The importance of internal (intraparticle) diffusion was evaluated from the Wheeler–Weisz (Φ) dimensionless number [52]:

$$\Phi = \eta \cdot \phi^2 = \left(\frac{(-r_{obs}) \cdot L^2}{D_{eff} \cdot C_{DCM0}} \right) < 0.15 \quad (3)$$

Table 2
Differential DCM molar balance in a fixed bed reactor.

Determining elementary step	Proposed kinetic expression
$DCM + l \leftrightarrow DCM$ Adsorption	$\frac{dx_{DCM}}{d\tau} = \frac{k_a \cdot C_{DCM0} \cdot (1-x_{DCM})}{1+K_S \cdot C_{DCM0} \cdot x_{DCM}}$
$DCMl \leftrightarrow Pl$ Surface reaction	$\frac{dx_{DCM}}{d\tau} = \frac{k_r \cdot C_{DCM0} \cdot (1-x_{DCM})}{1+K_A \cdot C_{DCM0} \cdot (1-x_{DCM}) + K_D \cdot C_{DCM0} \cdot x_{DCM}}$
$Pl \rightarrow P + l$ Desorption	$\frac{dx_{DCM}}{d\tau} = \frac{k_d \cdot C_{DCM0} \cdot (1-x_{DCM})}{1+K_Z \cdot C_{DCM0} \cdot (1-x_{DCM})}$

The values of *Da* and Φ fall well below 0.1 and 0.15, respectively, within the temperature range used in this work, thus allowing to neglect mass-transfer limitations in our experimental conditions according to the Carberry criteria [50].

To corroborate the absence of external and internal mass-transfer limitations two set of experiments were carried out at constant space time and 250 °C varying the gas velocity and the particle size of the catalyst within fairly wide ranges of 0.05–0.2 m s^{-1} and 0.15–0.7 mm, respectively. In these conditions, external and internal mass-transfer limitations were discarded since no significant differences in DCM conversion and product distribution were observed.

3.1. Pseudo-first order approach

Previous authors [47] used a pseudo-first order rate equation to predict the conversion of DCM in catalytic hydrodechlorination. We have checked this approach which incorporated into the mass-balance in a fixed bed reactor leads to:

$$\tau = \frac{W}{F_{DCM}} = \frac{1}{k \cdot C_{DCM0}} \cdot \ln(1 - x_{DCM})^{-1} \quad (4)$$

The dependence on the hydrogen concentration is included in the kinetic constant since a large excess of H_2 was used in all the experiments (H_2/DCM molar ratio = 100).

Fig. 1 shows the experimental values of $\ln(1-x_{DCM})^{-1}$ vs. τ which as can be observed, show significant deviations from this simple model. Fairly low values of the correlation coefficient (r^2) were obtained, especially as temperature increases (0.9 at 200 °C; 0.78 at 300 °C). The values of the kinetic constant ranged from 1.6 ± 0.2 (200 °C) to 16.4 ± 2.0 (300 °C) NL kg^{-1} h^{-1} and an apparent activation energy of 52.3 kJ mol^{-1} was calculated from the Arrhenius equation. A somewhat lower value of activation energy was obtained by Lopez et al. [47] (41.1 kJ mol^{-1}) working with Pd/Al_2O_3 in the 250–300 °C temperature range.

3.2. Models based on Langmuir–Hinshelwood (LH) mechanism

According to our previous work [43] the active centers of Pd/AC catalysts are constituted by the association of electron-deficient palladium (Pd^{n+}) where the chlorinated compound is adsorbed and zero-valent palladium (Pd^0) where H_2 is adsorbed and dissociated. Thus, we considered that DCM and H_2 adsorption takes place over two different types of active Pd sites. XPS analysis of the catalyst confirmed the presence of both Pd species in the commercial Pd/AC catalyst used in this work.

Table 2 shows the expressions resulting from the application of LH kinetic equations to the fixed bed reactor depending on the rate-controlling step. These equations were fitted to the experimental data by means of a non-linear least squares minimization procedure based on a modification of Powell's algorithm. The necessary mathematical tools are included in the commercial software Scientist 3.0 (Micromath Research) which implements the EPISODE package to solve the system of differential equations. The quality of the fit was evaluated from the correlation coefficient (r^2).

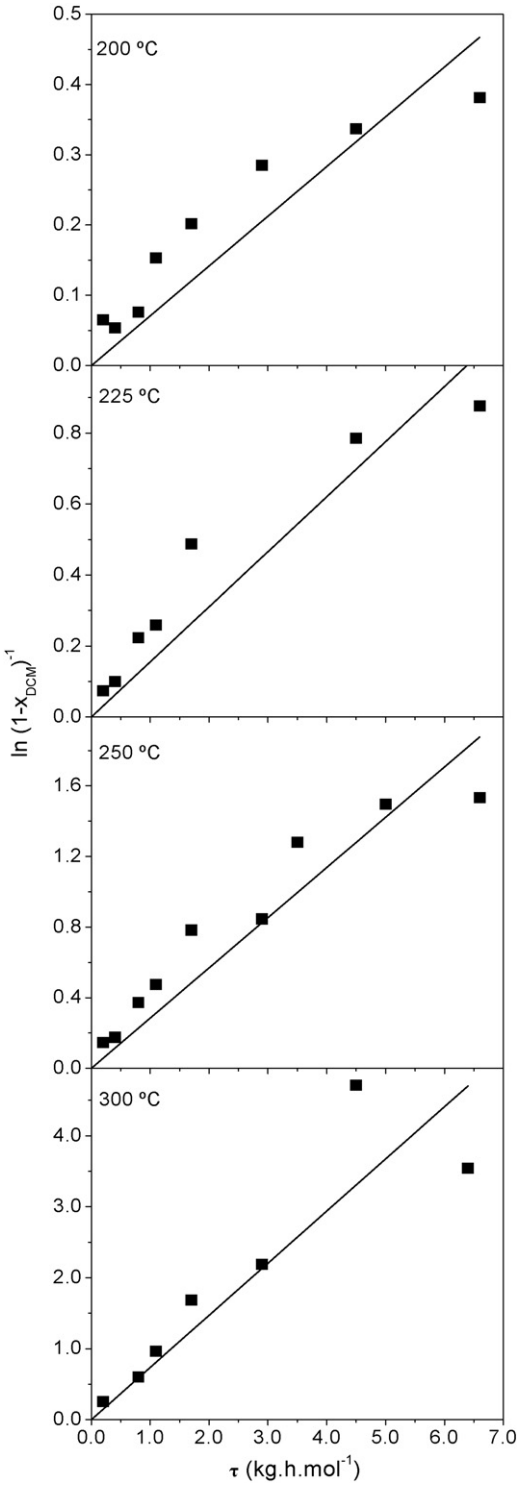

Fig. 1. Pseudo-first order plots for the HDC of DCM over Pd/AC catalyst at different temperatures.

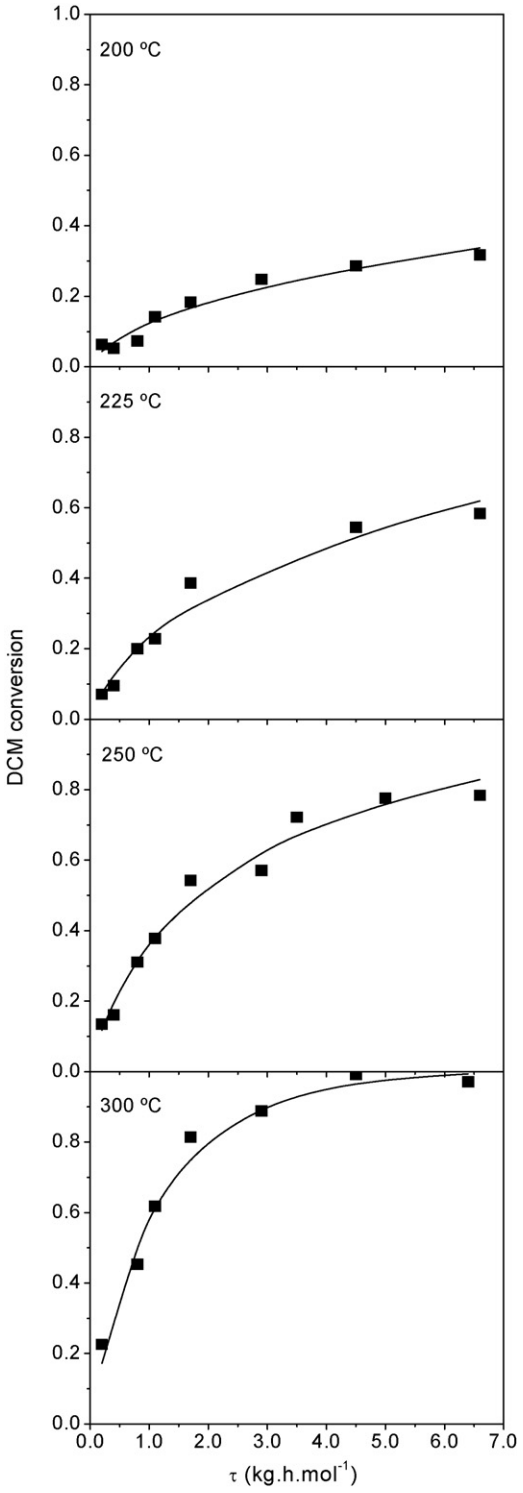

Fig. 2. DCM conversion vs. space time at different temperatures. Experimental values (symbols) and fitted curves for the LH model with DCM adsorption as rate-controlling step.

Although the fitting of the three LH models to the experimental data provided fairly good values of the correlation coefficient, only the one considering DCM adsorption onto the active sites as the rate-controlling step yielded reliable values of the parameters since in the two other cases negative values were obtained for some parameters (K_A, K_Z and at some temperatures K_D). Also, erratic values of the reaction rate constant (k_r) as a function of temperature were obtained for the LH model with chemical reaction as rate-controlling step.

Fig. 2 shows the experimental values of the DCM conversion vs. space time at different temperatures as well as the fitting curves for the LH model with adsorption as controlling step. As can be seen, this model provides a fairly good prediction of the experimental results. The values of the parameters are reported in Table 3.

Weiss and Krieger [53] also proposed the dissociative adsorption of chlorinated compounds as the rate-determining step for CCl_4 hydrodechlorination. A strong relationship between the strength

Table 3
Fitting parameters for the LH model with DCM adsorption as the rate-controlling step.

Temperature (°C)	$k_a \times 10^{-3}$(NL kg^{-1} h^{-1})	$K_S \times 10^{-3}$ (NL mol^{-1})	r^2
200	7.62 ± 5.13	557.78 ± 495.06	0.989
225	10.34 ± 3.98	136.0 ± 89.71	0.992
250	16.61 ± 5.02	75.78 ± 43.55	0.995
300	21.31 ± 4.67	6.27 ± 13.10	0.998

of the C–Cl bond and reactivity was found in the hydrodechlorination of CCl_4, $CHCl_3$ and CH_2Cl_2 [41,42] which is consistent with the assumption that the scission of the C–Cl bond accompanying to dissociative adsorption is the rate-determining step.

3.3. Reaction pathway

Fig. 3 shows the evolution of DCM concentration and the reaction products with space time at two different temperatures, 225 and 300 °C.

As can be observed conversion of DCM improves dramatically when increasing the temperature from 225 to 300 °C. At this last temperature methane, methyl chloride, ethane and ethylene were formed being methane by far the main reaction product at any space time tested, with selectivities higher than 70% in all the cases. Methyl chloride and ethane were formed in small amounts, and trace quantities of ethylene were only detected at low space times and 300 °C. At lower temperatures, ethylene was scarcely produced probably because it is rapidly hydrogenated to C_2H_6 on the surface of Pd [54]. Increasing the temperature slightly increases the selectivity to C2 hydrocarbons (C_2H_6 and C_2H_4) at the expense of methane.

Malinowski et al. [46] working with a Pd/Al_2O_3 catalyst at 140 °C obtained selectivities to CH_4, CH_3Cl and C_2H_6 of 69%, 31% and less than 1%, respectively, within the DCM conversion range of 0-10%. These authors did not detected C_2H_4, which can be explained on the basis of the low reaction temperature used in their experiments. Other authors [42] reported C_2H_4 formation at higher (>250 °C) reaction temperatures.

In order to elucidate the reaction pathway some hydrodechlorination experiments were carried out with CH_3Cl under the same reaction condition than for DCM. No significant conversion was achieved. In a previous work [43] we reported very low reactivity of monochloromethane with Pd/AC catalyst. In the same way, Malinowski et al. [46] proposed a reaction scheme from the results obtained upon DCM hydrodechlorination using D_2 instead of H_2 which considers that CH_3Cl readsorption can be ignored. This is consistent with the general trend observed for the reactivity of chloromethanes which decreases as the number of chlorine atoms of the molecule diminishes [42].

From the results obtained the process seems to occur via a parallel reaction scheme where CH_3Cl, CH_4 and C2 hydrocarbons (C_2H_6 and C_2H_4) are formed as primary products.

The reaction scheme of Fig. 4 is proposed for DCM hydrodechlorination. In that scheme the formation of the reaction products would take place from radical intermediates adsorbed on the active sites of the catalyst. CH_2Cl_2 would be dissociatively adsorbed at the Pd surface via C–Cl breaking yielding CH_3Cl or a carbene intermediate (CH_2^{**}). This adsorbed species would evolve to CH_4 through hydrogenation or to $C_2H_4^{**}$ through dimerization. Ethane and ethylene would be formed from the $C_2H_4^{**}$ intermediate, being the formation of both C_2 products considered coupled in a single step.

From the proposed mechanism, taking into account that the LH model with adsorption as controlling step describes fairly well the evolution of DCM concentration and assuming pseudo-first order kinetics for the other reaction steps, the net production rates (R_i) of the species involved in the process can be expressed as follows:

$$-R_{DCM} = r_1 = (-r_{DCM}) = \frac{k_1 \cdot C_{DCM}}{1 + K \cdot (C_{DCM0} - C_{DCM})} \quad (5)$$

$$R_{CH_2Cl^*} = r_1 - r_2 - r_3 = \frac{k_1 \cdot C_{DCM}}{1 + K \cdot (C_{DCM0} - C_{DCM})} - (k_2 + k_3) \cdot C_{CH_2Cl^*} \quad (6)$$

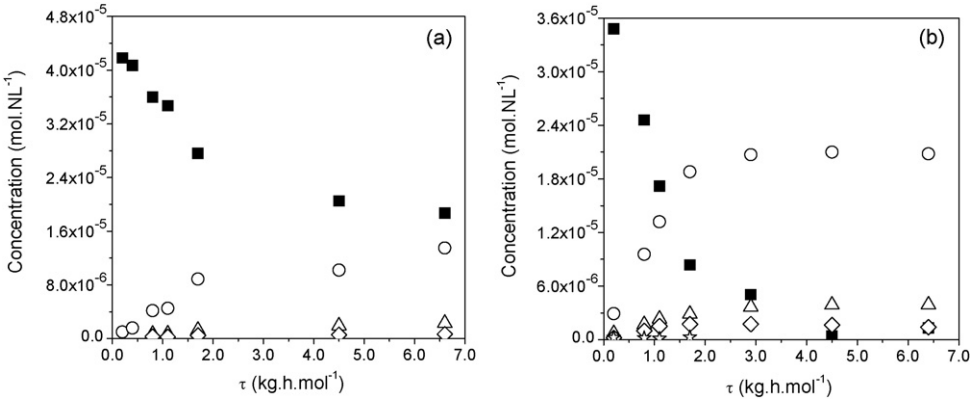

Fig. 3. Exit concentration of DCM (■), methane (○), monochloromethane (△), ethane (◊) and ethylene (☆) vs. space time at 225 °C (a) and 300 °C (b).

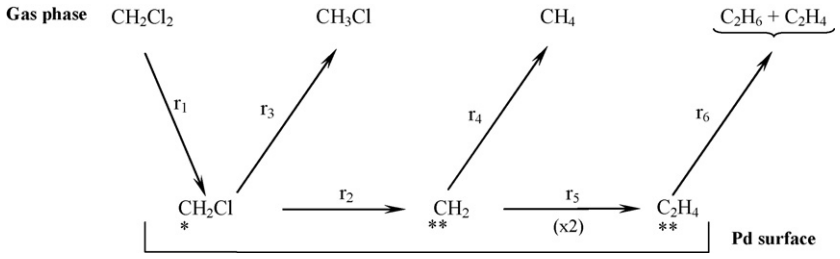

Fig. 4. Reaction scheme for HDC of DCM.

Table 4
Parameters of the kinetic model.

Temperature (°C)	$k_1 \times 10^{-3}$ (NL kg^{-1} h^{-1})	$K \times 10^{-3}$ (NL mol^{-1})	$k_{CH_4} \times 10^{-3}$ (NL kg^{-1} h^{-1})	$k_{CH_3Cl} \times 10^{-3}$ (NL kg^{-1} h^{-1})	$k_{C_2} \times 10^{-3}$ (NL kg^{-1} h^{-1})	r^2
200	6.98 ± 2.08	489.20 ± 201.10	3.03 ± 0.92	0.57 ± 0.17	0.11 ± 0.24	0.999
225	9.50 ± 1.71	117.42 ± 38.47	4.46 ± 0.83	0.75 ± 0.22	0.20 ± 0.26	0.997
250	14.00 ± 1.78	52.11 ± 15.52	7.14 ± 0.94	1.26 ± 0.21	0.47 ± 0.26	0.995
300	19.83 ± 1.94	1.11 ± 5.23	9.59 ± 0.99	1.71 ± 0.26	0.86 ± 0.30	0.993

$$R_{CH_3Cl} = r_3 = k_3 \cdot C_{CH_2Cl^*} \quad (7)$$

$$R_{CH_2{}^{**}} = r_2 - r_4 - r_5 = k_2 \cdot C_{CH_2Cl^*} - (k_4 + k_5) \cdot C_{CH_2{}^{**}} \quad (8)$$

$$R_{CH_4} = r_4 = k_4 \cdot C_{CH_2{}^{**}} \quad (9)$$

$$R_{CH_2CH_2{}^{**}} = r_5 - r_6 = k_5 \cdot C_{CH_2{}^{**}} - k_6 \cdot C_{CH_2CH_2{}^{**}} \quad (10)$$

$$R_{CH_3CH_3+CH_2CH_2} = r_6 = k_6 \cdot C_{CH_2CH_2{}^{**}} \quad (11)$$

where the stoichiometric coefficients are included in the corresponding kinetic constant (k_1–k_6).

On the basis of the steady state approximation the production rates of compounds identified can be expressed as:

$$-R_{DCM} = r_1 = (-r_{DCM}) = \frac{k_1 \cdot C_{DCM}}{1 + K \cdot (C_{DCM0} - C_{DCM})} \quad (12)$$

$$R_{CH_3Cl} = r_3 = \frac{k_{CH_3Cl} \cdot C_{DCM}}{1 + K \cdot (C_{DCM0} - C_{DCM})} \quad (13)$$

$$R_{CH_4} = r_4 = \frac{k_{CH_4} \cdot C_{DCM}}{1 + K \cdot (C_{DCM0} - C_{DCM})} \quad (14)$$

$$R_{C_2} = r_6 = \frac{k_{C_2} \cdot C_{DCM}}{1 + K \cdot (C_{DCM0} - C_{DCM})} \quad (15)$$

where

$$k_{CH_4} = \frac{k_1 \cdot k_2 \cdot k_4}{(k_2 + k_3) \cdot (k_4 + k_5)}$$

$$k_{CH_3Cl} = \frac{k_1 \cdot k_3}{(k_2 + k_3)}$$

$$k_{C_2} = \frac{k_1 \cdot k_2 \cdot k_5}{(k_2 + k_3) \cdot (k_4 + k_5)}$$

Then, from the molar balance in a fixed bed reactor, the following expressions were obtained:

$$\frac{dC_{DCM}}{d\tau} = C_{DCM0} \cdot \left(-\frac{k_1 \cdot C_{DCM}}{1 + K \cdot (C_{DCM0} - C_{DCM})} \right) \quad (16)$$

$$\frac{dC_{CH_3Cl}}{d\tau} = C_{DCM0} \cdot \left(\frac{k_{CH_3Cl} \cdot C_{DCM}}{1 + K \cdot (C_{DCM0} - C_{DCM})} \right) \quad (17)$$

$$\frac{dC_{CH_4}}{d\tau} = C_{DCM0} \cdot \left(\frac{k_{CH_4} \cdot C_{DCM}}{1 + K \cdot (C_{DCM0} - C_{DCM})} \right) \quad (18)$$

$$\frac{dC_{C_2H_6+C_2H_4}}{d\tau} = C_{DCM0} \cdot \left(\frac{k_{C_2} \cdot C_{DCM}}{1 + K \cdot (C_{DCM0} - C_{DCM})} \right) \quad (19)$$

As before, the system of differential equations were simultaneous fitted to the experimental data by means of the non-linear least square procedure provided by the commercial software Scientist 3.0 (Micromath Research). Fig. 5 shows the experimental concentration vs. space time values obtained together with the fitting curves. The values of the parameters and correlation coefficients are given in Table 4. As can be seen the model describes fairly well the experimental results.

Table 5 shows the ratio between the kinetic constants associated with the formation of the different reaction products and that

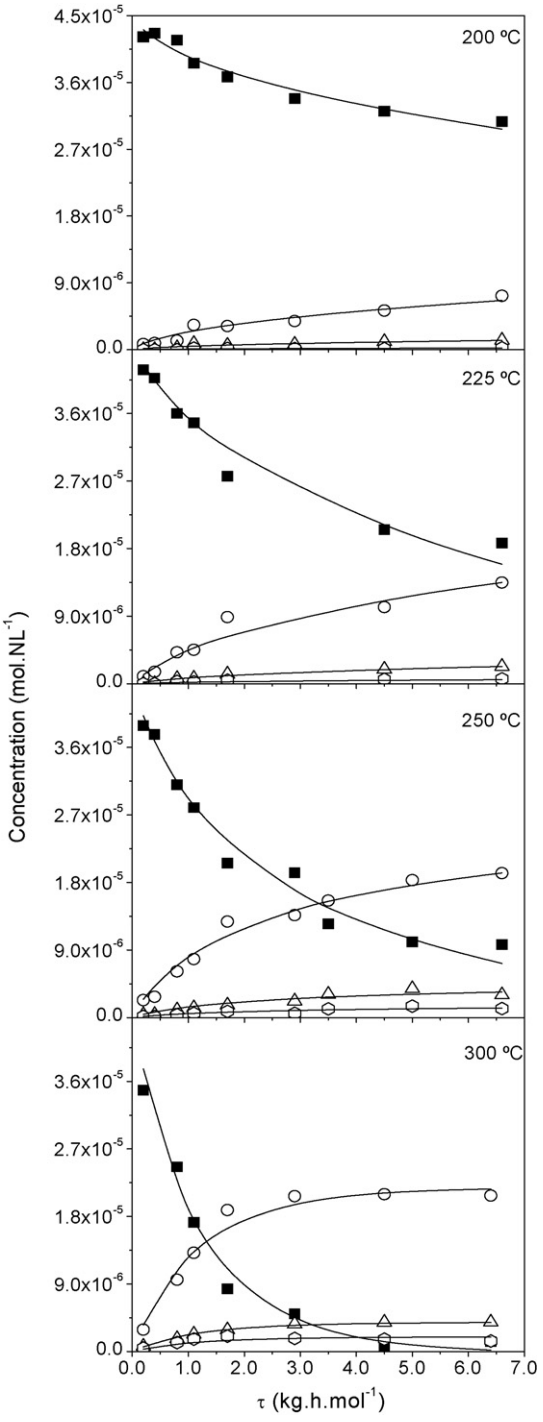

Fig. 5. Experimental (symbols) and predicted (lines) concentrations of DCM (■), methane (○), monochloromethane (△), ethane and ethylene (○) at different temperatures.

Table 5
Relation between the kinetic constants of products formation and DCM disappearance.

Temperature (°C)	k_{CH_4}/k_1	k_{CH_3Cl}/k_1	k_{C_2}/k_1
200	0.434	0.082	0.015
225	0.469	0.079	0.021
250	0.510	0.090	0.034
300	0.484	0.086	0.043

of DCM disappearance. As can be seen that ratio does not undergo significant variations with temperature except in the case of C_2 formation which shows a monotonical increase within the range investigated. This suggests that $C_2H_4^{**}$ formation through CH_2^{**} dimerization on the catalyst surface is favoured by increasing the temperature. This is in agreement with the results obtained by Mori et al. [42], who found that the probability of chain-growth increases with the reaction temperature and with the reactivity of chloromethanes ($CCl_4 > CHCl_3 > CH_2Cl_2$).

The apparent activation energy (Ea) for DCM disappearance was calculated on the basis of the Arrhenius equation applied to k_1 since this kinetic constant does not include any adsorption parameter. A value of $23.9 \pm 2.3\,kJ\,mol^{-1}$ was obtained within 95% confidence limits. Lopez et al. [44] and Sanchez et al. [48] have reported values of $\sim 41\,kJ\,mol^{-1}$ and $22–30\,kJ\,mol^{-1}$, respectively, with Pd/Al_2O_3 catalysts for the same reaction. Likewise, several studies focused on the hydrodechlorination of chlorinated alkanes in gas-phase over Pd catalysts reported Ea values in the same range than the obtained in this work [55–59].

4. Conclusions

The kinetics of DCM hydrodechlorination with a Pd on activated carbon catalyst has been studied in a fixed bed reactor in absence of mass-transfer limitations. The Langmuir–Hinshelwood model with DCM adsorption as the rate-controlling step describes fairly well the experimental results.

From the evolution of DCM and the reaction products a reaction pathway has been proposed based on the formation of adsorbed intermediates (CH_2Cl^* radical, CH_2^{**} carbene and $C_2H_4^{**}$ species) which yield CH_4, CH_3Cl, C_2H_6 and C_2H_4.

Using the aforementioned LH model for DCM disappearance and assuming pseudo-first-order dependence for the other reaction steps, a kinetic model describing the evolution of all the species identified has been proposed and validated. An apparent activation energy of $23.9 \pm 2.3\,kJ\,mol^{-1}$ has been obtained for DCM disappearance.

Acknowledgments

The authors acknowledge financial support from the Spanish MEC through the project CTQ2005-07579PPQ.

References

[1] USEPA 2001, Toxic release inventory, Public data release report, Office of Pollution Prevention and Toxics, U.S. Environmental Protection Agency, Washington, DC, 2003.
[2] W.J. Hayes Jr., E.R. Laws Jr. (Eds.), Handbook of Pesticide Toxicology, vol. 1, General Principles, Academic Press, San Diego, 1991.
[3] E. Dobrzynska, M. Posniak, M. Szewczynska, B. Buszewski, Crit. Rev. Anal. Chem. 40 (2010) 41–57.
[4] N.P. Cheremisinoff, Industrial Solvents Handbook, 2nd ed., Marcel Dekker Inc., New York, 2003.
[5] A. Converti, M. Zilli, D.M.D. Faveri, G. Ferraiolo, J. Hazard. Mater. 27 (1991) 127–135.
[6] T.N. Kalnes, R.B. James, Environ. Prog. 7 (1988) 185–191.
[7] B.H. Carpenter, D.L. Wilson, J. Hazard. Mater. 17 (1988) 125–148.
[8] F.W. Karasek, R.E. Clement, A.C. Viau, J. Chromatogr. 239 (1982) 173–180.
[9] B. Coq, G. Ferrat, F. Figueras, J. Catal. 101 (1986) 434–445.
[10] B. Heinrichs, P. Delhez, J.P. Schoebrechts, J.P. Pirard, J. Catal. 172 (1997) 322–335.
[11] R. Gopinath, N.S. Babu, J.V. Kumar, N. Lingaiah, P.S.S. Prasad, Catal. Lett. 120 (2008) 312–319.
[12] C. Amorim, M.A. Keane, J. Colloid Interface Sci. 322 (2008) 196–208.
[13] T. Mori, T. Yasuoka, Y. Morikawa, Catal. Today 88 (2004) 111–120.
[14] T. Yoneda, T. Takido, K. Konuma, Appl. Catal., B 84 (2008) 667–677.
[15] E. Trabuco, P.C. Ford, J. Mol. Catal. A: Chem. 148 (1999) 1–7.
[16] Y. Mitoma, M. Takase, Y. Yoshino, T. Masuda, H. Tashiro, N. Egashira, T. Oki, Environ. Chem. 3 (2006) 215–218.
[17] M. Makkee, A. Wiersma, E. van de Sandt, H. van Bekkum, J.A. Moulijn, Catal. Today 55 (2000) 125–137.
[18] C.J. Noelke, H.F. Rase, Ind. Eng. Chem. Prod. Res. Dev. 18 (1979) 325–328.
[19] M. Legawiec-Jarzyna, A. Srebowata, W. Juszczyk, Z. Karpinski, J. Mol. Catal. A: Chem. 224 (2004) 171–177.
[20] J.W. Bae, J.S. Lee, K.H. Lee, Appl. Catal. A 334 (2008) 156–167.
[21] A. Wiersma, E.J.A.X.v.D. Sandt, M.A.D. Hollander, H.V. Bekkum, M. Makkee, J.A. Moulijn, J. Catal. 177 (1998) 29–39.
[22] C.D. Thompson, R.M. Rioux, N. Chen, F.H. Ribeiro, J. Phys. Chem. B 104 (2000) 3067–3077.
[23] M. Gurrath, T. Kuretzky, H.P. Boehm, L.B. Okhlopkova, A.S. Lisitsyn, V.A. Likholobov, Carbon 38 (2000) 1241–1255.
[24] L.R. Radovic, C. Moreno-Castilla, J. Rivera-Utrilla, Carbon Materials as Adsorbents in Aqueous Solutions. Chemistry and Physics of Carbon, Marcel Dekker, New York, 2000.
[25] G. Tavoularis, M.A. Keane, J. Mol. Catal. A: Chem. 142 (1999) 187–199.
[26] S.B. Halligudi, B.M. Devassay, A. Ghosh, V. Ravikumar, J. Mol. Catal. A: Chem. 184 (2002) 175–181.
[27] R. Gopinath, N. Lingaiah, N.S. Babu, I. Suryanarayana, P.S.S. Prasad, A. Obuchi, J. Mol. Catal. A: Chem. 223 (2004) 289–293.
[28] E. Lopez, S. Ordoñez, F.V. Diez, Appl. Catal., B 62 (2006) 57–65.
[29] Y. Mitoma, N. Egashira, C. Simion, Chemosphere 74 (2009) 968–973.
[30] D.A. Dodson, H.F. Rase, Ind. Eng. Chem. Prod. Res. Dev. 17 (1978) 236–241.
[31] M. Martino, R. Rosal, H. Sastre, F.V. Diez, Appl. Catal., B 20 (1999) 301–307.
[32] E.S. Lokteva, V.I. Simagina, E.V. Golubina, I.V. Stoyanova, V.V. Lunin, Kinet. Catal. 41 (2000) 776–781.
[33] Y.H. Choi, W.Y. Lee, J. Mol. Catal. A: Chem. 174 (2001) 193–204.
[34] B. Heinrichs, F. Noville, J.P. Schoebrechts, J.P. Pirard, J. Catal. 220 (2003) 215–225.
[35] S. Lambert, J.F. Polard, J.P. Pirard, B. Heinrichs, Appl. Catal., B 50 (2004) 127–140.
[36] J. Halasz, M. Hodos, I. Hannus, G. Tasi, I. Kiricsi, Colloids Surf., A 265 (2005) 171–177.
[37] M. Legawiec-Jarzyna, A. Srebowata, W. Juszczyk, Z. Karpinski, React. Kinet. Catal. Lett. 87 (2006) 291–296.
[38] M. Bonarowska, A. Malinowski, Z. Karpinski, Appl. Catal., A 188 (1999) 145–154.
[39] L. Prati, M. Rossi, Appl. Catal., B 23 (1999) 135–142.
[40] B. Aristizabal, C.A. Gonzalez, I. Barrio, M. Montes, C.M. de Correa, J. Mol. Catal. A: Chem. 222 (2004) 189–198.
[41] S. Ordoñez, H. Sastre, F.V. Diez, Appl. Catal., B 25 (2000) 49–58.
[42] T. Mori, K. Hirose, T. Kikuchi, J. Kubo, Y. Morikawa, J. Jpn. Pet. Inst. 45 (2002) 256–259.
[43] Z.M. de Pedro, L.M. Gomez-Sainero, E. Gonzalez-Serrano, J.J. Rodriguez, Ind. Eng. Chem. Res. 45 (2006) 7760–7766.
[44] E. Lopez, S. Ordoñez, F.V. Diez, Catal. Today 84 (2003) 121–127.
[45] C.A. Gonzalez, M. Bartoszek, A. Martin, C.M. de Correa, Ind. Eng. Chem. Res. 48 (2009) 2826–2835.
[46] A. Malinowski, D. Lomot, Z. Karpinski, Appl. Catal., B 19 (1998) L79–L86.
[47] E. Lopez, S. Ordoñez, H. Sastre, F.V. Diez, J. Hazard. Mater. 97 (2003) 281–294.
[48] C.A.G. Sanchez, C.O.M. Patino, C.M. de Correa, Catal. Today 133 (2008) 520–525.
[49] C. Perego, S. Peratello, Catal. Today 52 (1999) 133–145.
[50] J.J. Carberry, Chemical and Catalytic reaction Engineering, in: Chemical Engineering Series, McGraw Hill, New York, 1976.
[51] N. Frössling, Gerlands Beitr. Geophys. 52 (1938) 170–175.
[52] P.B. Weisz, D.C. Prater, Advances in catalysis, in: Interpretation of Measurements in Experimental Catalysis, vol. 6, Academic Press, New York, 1954.
[53] A.H. Weiss, K.A. Krieger, J. Catal. 6 (1966) 167–185.
[54] S. Ordoñez, F.V. Diez, H. Sastre, Ind. Eng. Chem. Res. 41 (2002) 505–511.
[55] B. Heinrichs, J.P. Schoebrechts, J.P. Pirard, J. Catal. 200 (2001) 309–320.
[56] T. Mori, J. Kubo, Y. Morikawa, Appl. Catal., A 271 (2004) 69–76.
[57] A. Malinowski, W. Juszczyk, M. Bonarowska, J. Pielaszek, Z. Karpinski, J. Catal. 177 (1998) 153–163.
[58] N. Chen, R.M. Rioux, F.H. Ribeiro, Appl. Catal., A 271 (2004) 85–94.
[59] A. Srebowata, W. Juszczyk, Z. Kaszkur, Z. Karpinski, Catal. Today 124 (2007) 28–35.